ISSN : 0974 - 7486 Volume 11 Issue 6

Materials Science

An Indian Journal

Full Paper

MSAIJ, 11(6), 2014 [225-232]

Nanostructured nickel-based composite thin film reinforced with graphite and different SiC nanoparticles

Abbas Fahami*, Bahman Nasiri-Tabrizi

Materials Engineering Department, Najafabad Branch, Islamic Azad University, Najafabad, Isfahan, (IRAN)

E-mail: ab.fahami@gmail.com

ABSTRACT

In this study, nickel- based nanocomposite coatings were prepared from a Watts type electrolyte containing reinforcement's particles (silicon carbide and graphite) to deposit on steel St-37 substrate. For these purposes, the adding of different SiC concentrations in electrolyte (g/l) affecting on microhardness of nanocomposite coating was investigated to optimize high quality coatings with appropriate microhardness and morphological features. Based on XRD results, the main peaks in the samples were nickel and SiC phases. Microscopic observations illustrated a cluster like structure which consisted of some fine sphere particles with an average particle size of about 62 nm. The outcomes revealed that the greater amount of SiC in bath solution resulted in much more absorbance of reinforcement particulates into coatings and consequently prepare a harder surface. The hardness of the coatings was also measured and found to be 529 to 630 (Hv) depending on the electrolyte concentrations and the reinforcements weight percentage (wt.%) in the nickel-based thin film. According to the elemental mapping spectra, a homogenous distribution of nickel, silicon and carbon particles was appeared into the nickel-based coatings. Ultimately, the experimental outcomes demonstrated that various bath concentrations had considerable influences on microhardness and morphology properties of the Ni–SiC–Gr coatings.

KEYWORDS

Electrochemical method;
Nanocomposite thin film;
Microhardness;
Electron microscopy (SEM/ FE-SEM).

INTRODUCTION

Recently, the promotion of low carbon steel (St–37) surfaces was evaluated by numerous investigators so that researches and developments on Ni based composite coatings have come into prominence which can meet the industrial request[1-4]. It was proved that the uniform dispersion of the codeposited particles such as Ni, Pd, Cu, NiP, Ni–W and Ni–Fe–Cr leads to the improvement of mechanical and the tribological properties of parts surface[5,6]. For coatings preparation, several methods such as electrodeposition, ion implantation, chemical vapor deposition (CVD), laser beam deposition, physical vapor deposition (PVD), plasma and high-velocity oxygen fuel (HVOF) spraying have been served[7,8]. The electrochemical deposition of nano-size particles in a metallic matrix has led to a new generation of composites due to the advantages of this technique. The easy maintainability, easy low working temperatures, low cost and high production rate are

the remarkable features of this method[9].

In chemical techniques, the optimum electrochemical parameters have been used to absorb the fine particles on the surface. In this approach, the repulsion force between particles with the same charges can be increased. This, in turn, reduces the agglomeration and provides a solution with more stable particles. The use of nano-size particles in coatings could be declined the problem of created imperfection such as voids between the particles and matrix interfaces. In addition, the deposition of enough amounts of reinforced particles could lead to generation of stronger and more resistant covers. Also, electrodeposition as an appropriate procedure was proposed to facilitate deposition of fine particulates on the low carbon steel surface. Nickel matrix coatings have received widespread acceptance as it provides a uniform deposit on irregular surfaces, direct deposition on surface activated, high hardness and excellent resistance to wear, abrasion and corrosion. Additionally, nickel as an engineering material was broadly used among the electrodeposited surfaces[10]. Several studies were demonstrated that deposition of coatings in the presence of fine particles such as a hard materials (ceramics particles) or lubricating particles (PTFE and graphite (Gr)) into the Ni based, might effectively improve the mechanical and tribological properties of the surfaces[11-21]. Research on electrodeposition of nanocomposite coatings has been directed towards the determination of optimum conditions for their production, i.e. bath temperature, pH value, stirring speed, current density and particles concentration in electrolyte. Meanwhile, by manipulating the processing parameters some remarkable results were acquired[22]. It should be noted that the choosing of optimum circumstances for production of nickel coatings from the reported results is difficult because they are, in some cases, different or paradoxical[23].

The electrochemical parameters are very effective in electrochemical deposition of coatings in presence of reinforcement particles (silicon carbide (SiC) and graphite (Gr)), therefore obtaining of precise determination of these parameters with proper microhardness was the main target of this paper. Thus, the influence of bath concentration on the morphological and microhardness characteristics of Ni–SiC–Gr nanocomposite coatings was investigated. In addition, a comparison study of the properties of these coatings at different conditions was conducted. Therefore, the optimum condition of bath solutions with different SiC values in electrolyte was evaluated by X–ray diffraction (XRD), field emission scanning electron microscopy (FE–SEM), scanning electron microscopy (SEM), energy dispersive X–ray spectroscopy (EDS) and Elemental mapping analysis. Moreover, the microhardness of specimens was measured by Micro hardness Tester, as a result the outcomes showed remarkable consequences.

EXPERIMENTAL PROCEDURES

Electrodeposition of Ni based nanocomposite coatings

Nickel based coatings were deposited from Watts bath by direct current (DC) electroplating. The basic components of the electrolyte were consisted of nickel sulfate (Merck, 99%), boric acid (Merck, 99.8%) and nickel chloride (Merck, 98%). The plating compositions and the experimental operating parameters are shown in TABLE 1. Silicon Carbide (SiC) (Hefeikaier Nanometer Energy & Technology, 99%) and graphite (Gr) (Merck, 99.8%) with the average crystallite size 40 – 100 nm and 5 – 100 μm were used in the experiments as the reinforcing phases, respectively. The surfactants such as cetyltrimethylammonium bromide (CTAB, Merck 98%), sodyumdodecyl sulfate (SDS, Acros Organics 98%) and Saccharine (Merck 99%) were utilized to increase the electrostatic adsorption of suspended particles on the cathode surface by enhancement of their positive charge[24]. In the electrodeposition experiments, in order to determine the influence of SiC concentrations in the electrolyte on the weight percentage (wt.%) of the SiC in the plated layer, the con-

TABLE 1 : Overview of electrochemical plating conditions

Bath composition (g/l)		Operating conditions	
$NiSO_4.6H_2O$	200	Temperature (T °c)	45
$NiCl_2.6H_2O$	20	pH	4.8
H_3BO_3	40	Current density (A/ dm^2)	4
SiC	9–12–15–18	Stirring speed (rpm)	500
Graphite	1	Plating time (min)	20
CTAB	5	Electrolyte volume (cc)	100
SDS	5	Anode	Ni
$C_7H_5NO_3S$	1	Cathode	St-37

tent of the SiC was varied from 9 to 18 g/l. The plating conditions were a bath temperature of 45 °C, a rpm of 500, a pH of 4.8, and a current density of 4 A/dm^2. The electrochemical plating of all the specimens was performed for 20 min by magnetite stirring for each electroplating run. Furthermore, the sonication process time was 15 min to provide homogeneous dispersion and to prevent agglomeration of the particles.

Low carbon steel (St–37) plates with dimensions of 10 mm × 10 mm × 1 mm were used as the substrate (cathode) and also nickel cylindrical was utilized as a anode for electroplating process. In brief, the preparation of the specimen's surfaces was carried out at three stages; degreasing, acid pickling and polishing. After each step, the plates have been rinsed by distilled water to remove the residuals of each stage, completely.

Characterization of electrodeposited Ni based nanocomposite coatings

Phase analyses and structural changes of deposited layers were determined by X–ray diffraction (Philips X–ray diffractometer (XRD), *Cu–K*$_\alpha$ radiation, 40 kV, 30 mA and 0.02 ° S^{-1} step scan). For qualitative analysis, XRD graphs were recorded in the interval 20° d" 2θ d" 70° at scan speed of 1°/min. This range covers two strongest peaks of nickel and also two peaks of SiC. "*PANalytical X'Pert HighScore*" software was also utilized for the analysis of different peaks. The gained patterns were compared to standards compiled by the Joint Committee on Powder Diffraction and Standards (JCPDS), which involved card #04–0850 for Ni, #029–1128 for SiC and #047–1049 for NiO. The morphologies of coatings surfaces were observed by scanning electron microscopy (SEM, VEGA Tescan easyprobe). X–ray energy dispersion spectroscopy (EDS) and Elemental mapping analysis system which were coupled with SEM were utilized to determine the weight percentage of nanoparticles and distribution of particles (voltage used for EDX equal to 20 kV). The weight percentages of particles were measured at three different locations at same magnification of the images. The mean values are reported along with positive and negative error bars. A field emission scanning electron microscope (FE–SEM Hitachi S1831) that operated at the acceleration voltage of 15 kV was served to measure the particulates size and thickness of the thin layers. For this purpose, the plate's surfaces were coated with gold for more electronic conduction. A Vickers micro-hardness tester (MICROMET3, Buehler Ltd.USA) with Vickers pyramidal diamond indenter was served to analyze microhardness of the layers polished at room temperature. A load of 50 (g) was performed for 20 s and the final value quoted for the hardness of the deposit was the average of at least three measurements. It should be noted that the reported values of the microhardness are representative of the deposited coatings without significant influence from underlying substrate.

RESULTS AND DISCUSSIONS

XRD analysis

Figure 1 shows the X–ray diffractions of Ni–SiC–Gr nanocomposite coatings deposited at different bath solutions. The profiles of the samples confirm the presence of Ni, SiC, graphite (Gr) and NiO phases and no characteristic peaks of other phases have been recorded. Also, the presence of NiO as an extra phase demonstrates that the surface of the Ni based was oxidized during contacting with the plating bath[25]. Note that the peaks corresponding to Gr particles could not be completely identified in the XRD patterns from nanocomposite coatings due to very low content (1 g/L). Figure 1 also illustrates the profiles of the Ni and SiC peaks at different SiC concentrations in electrolyte. It can be seen that the intensity of SiC peaks are increased by rising of SiC contents in the bath. All the XRD patterns at different conditions display typical peaks corresponding to (111) and (200) crystallographic planes of nickel as well as the (102) and (110) planes of SiC. It has been reported that the embedding of SiC nano-particles in the Ni based could be modified the Ni texture from the soft [1 0 0] mode to the mixed preferred [2 1 1] orientation[26]. For all the deposited coatings at various electrochemical parameters, the intensity of the (111) peaks is higher than the other planes. This result indicated that the preferred orientation of Ni is (111) plane. It should be mentioned that the (111) peak at 2θ = 44.508° is the strongest peak (relative intensity = 100 %) in the standard XRD pattern from randomly oriented polycrystalline nickel

Full Paper

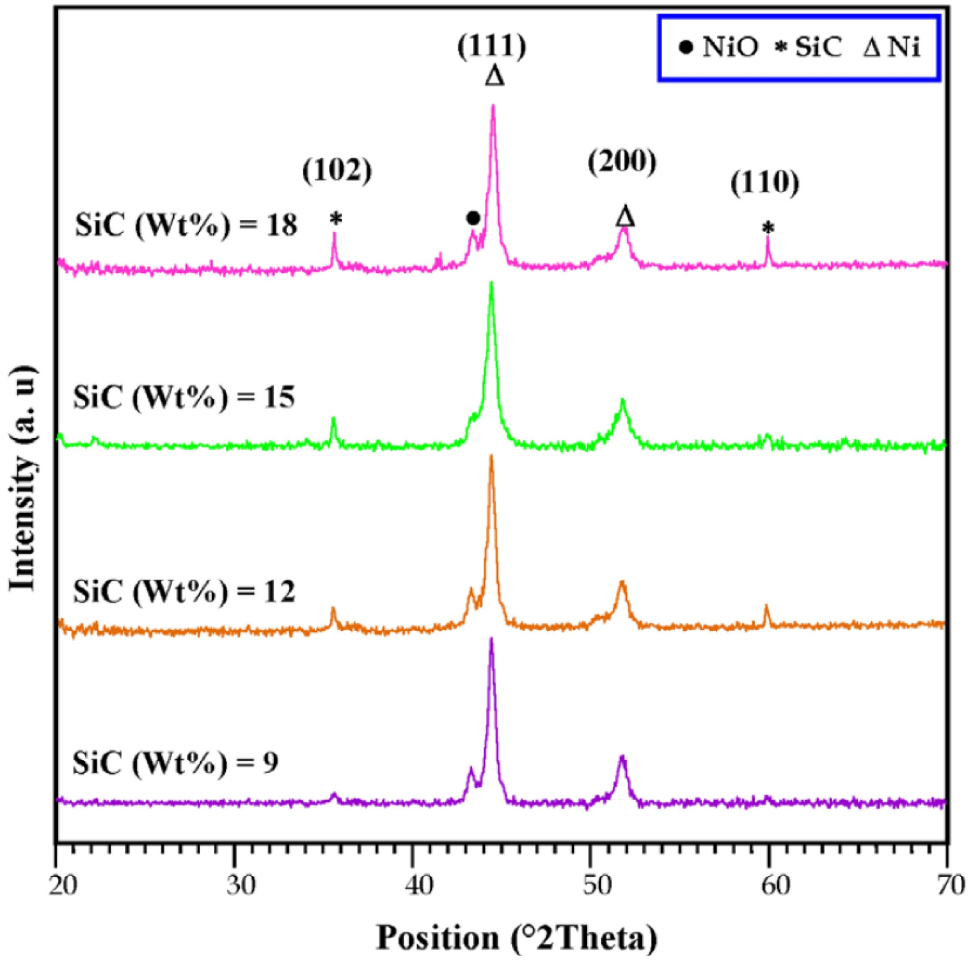

Figure 1 : XRD patterns of Ni–SiC–Gr nanocomposite coatings deposited at diverse SiC concentrations in electrolyte

(No. 04–0850). The crystallite size (D) for nickel composite coatings was calculated using Scherrer equation[27]:

$$\text{FWHM} = \frac{K\lambda}{D\cos\theta}\frac{180°}{\pi} \quad (1)$$

where FWHM is full width half maxima in 2θ degrees, D is the crystallite size in nm, K is constant (usually evaluated as 0.94), and λ is the wavelength of Cu Kα radiation (0.154 nm). The crystallinity percentage (Crl) of Ni phase for all the samples was determined by using the XRD data according to the following equation[28]:

$$\text{Crl} = \frac{I_{111} - I_{\alpha m}}{I_{111}} \times 100 \quad (2)$$

where I_{111} is the diffraction intensity of (111) plane and I_{am} is the intensity of the measured amorphous peak. Also, as a part of structural characteristics, the influence of bath parameters on Ni lattice (cubic) parameter constant (a_c) was evaluated by the equation[29]:

$$d_{hkl} = \frac{a_c}{\sqrt{(h^2 + k^2 + l^2)}} \quad (3)$$

where the Miller indices ($h\,k\,l$) obtained from the diffraction spectra were identified using JCPDS cards (No. 04-0850) and d_{hkl} is the distance between adjacent Bragg planes. TABLE 2 shows the crystallite sizes (nm), crystallinity (%) and lattice parameter (Å) of Ni phase for all the nanocomposite coatings calculated using FWHM of prominent (111) and (200) reflection in Scherrer equation.

TABLE 2 : Crystallite size, crystallinity and lattice parameter of nickel in nanocomposite coatings

	SiC in electrolyte (g/l)			
	9	**12**	**15**	**18**
D (nm)	21.8	20.3	20	19.96
Crl (%)	87.5	84.4	82.8	81.2
a_c (Å)	3.515	3.526	3.531	3.523

According to the TABLE 2, it can be seen that the crystallite size and crystallinity of nickel decreased by increasing of SiC values in the electrolyte. High crystalline Ni based coating was also obtained after addition of 9 g/l SiC into the bath; so, the crystallite size and crystallinity of nickel were 21.8 and 87.5, respectively. Eventually, it seems that the greater amount of SiC in electrolyte (9–18 g/l) leads to nickel-based coatings with lower crystallinity. It should be mentioned that the growth of coatings is controlled both by the nucleation and crystal growth rate. In the electrodeposition process, reinforcement's nanoparticles that adhere to the cathode surface act as nucleation sites and hence accelerate Ni based nucleation. During the process of electrocrystallization, grain nucleation and crystal growth occur simultaneously and are competitive[30]. The lattice parameter values for all the samples are close to the standard value ((# 04-0850: a=3.5228 Å) which indicates that different bath solutions affect less on the lattice constant of Ni.

SEM and FE-SEM observations

Figure 2 shows the surfaces morphology of Ni–SiC–Gr nanocomposite coatings deposited at different bath solutions. As can be seen, a cluster like structure containing of fine gains as well as some agglomerates were deposited on St–37 substrates at different SiC content in electrolyte (9 to 18 g/l). It can be seen that all the specimens have not regular surfaces so that there were much more pores in samples especially the specimen which were included smallest SiC contents in solution (9 g/l). It could be observed that some the reinforced particulates with cluster like structure are accompanied by some agglomerates dispersed into the nickel-based coating. Also, it seems that SiC and Gr particles were homogeneously incorporated in thin films, so that the increasing of SiC contents in the bath led to high adsorption of SiC into the matrix. Thus, it seems that the sample electrodeposited by 18 (g/l) SiC in the bath has optimum condition rather than the other coatings.

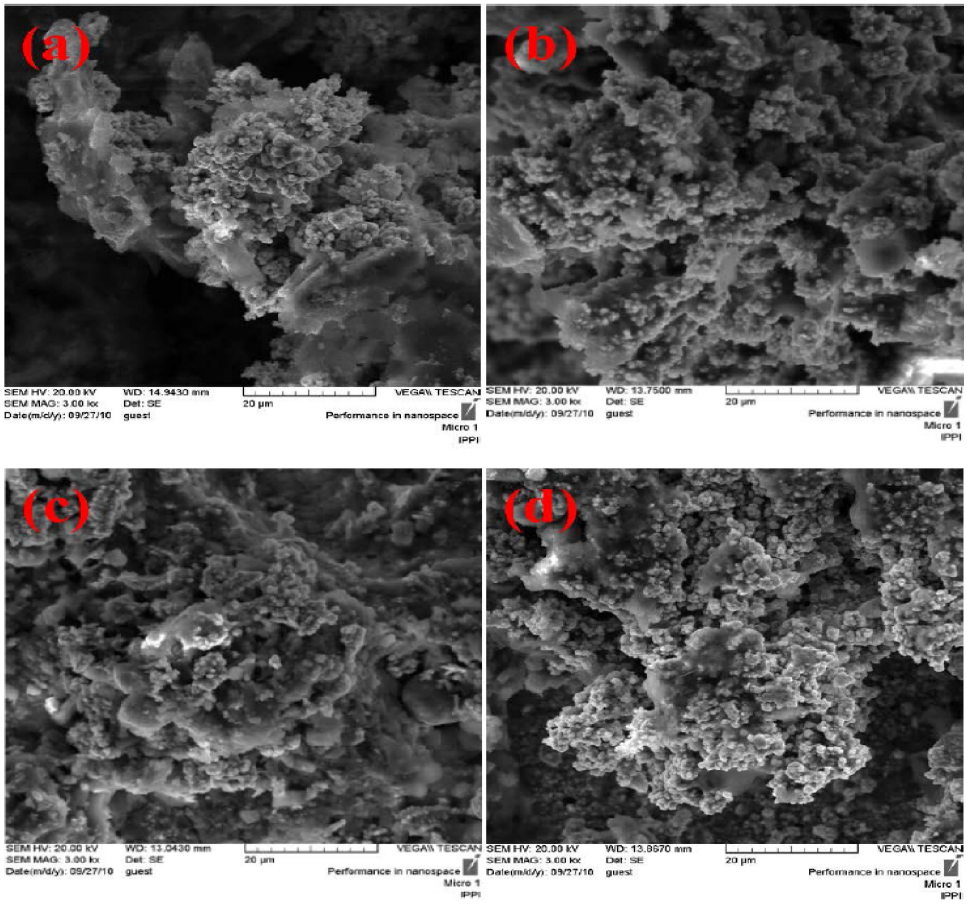

Figure 2 : SEM micrographs of Ni–SiC–Gr nanocomposite coatings deposited at different SiC concentrations in electrolyte (9, 12, 15, and 18 g/l)

Full Paper

The cross-sectional images of Ni–SiCGr nanocomposite coatings deposited at various bath solutions is shown in Figure 3. As can be seen, all the coatings deposited at various SiC values (9 to 18 g/l) in electrolyte were uniform and homogenous with a good bonding to the substrate. From higher magnification of FE-SEM observations, it is observed that Ni–SiC–Gr nanocomposite coatings were formed as spherical globules with the average crystallite size of 62 nm. It seems that the globules have tendency to adhere on clean upper surface of the substrate (St–37). The thickness of Ni based nanocomposite coatings produced at various bath solutions declined by rising SiC values in electrolyte and reached a minimum of 99 μm in case of 18 (g/l) in bath solution. It seems that SiC particles in the composite coatings act as physical barriers to grain growth and slow down the growth rate (hence thinner composite coatings). While hydrogen evolution at the cathode can also result in coating thickness reduction, such effects are not of electrodeposition from watts bath. Furthermore, boric acid in the electrolyte is known for suppressing the hydrogen evolution during electrodeposition of nickel from watts bath. The result is in agreement with other research[31].

EDS and elemental mapping analysis

The EDS (Energy dispersive X-ray spectroscopy) spectra of Ni–SiC–Gr nanocomposite coatings deposited at different bath solutions with 9, 12, 15, and 18 g/l SiC contents in electrolyte is shown in Figure 4. The results confirm the presence of Ni, Si, C, and O elements in the nanocomposites. Since, there is no specific separation in this analysis between carbon of graphite and carbide structures, the displayed carbon signals derived from silicon carbide and graphite sources. Furthermore, it is noteworthy to mention that chemically stable contaminants were not detected and also it demonstrates that the Ni–SiC–Gr nanocomposite coatings on St–37 have acceptable purity. According to Elemental mapping analysis, the distribution of reinforced materials such as SiC and Gr as well as Ni particles is depicted (see Figure 4), the dispersion of particles is uniformly homogenous in the samples. It seems that the attendance of reinforcement's particulates resulted in the changing of surface charges on the substrate and affected the deposition rate[32]. Therefore, determination of optimal bath parameters of electrochemical plating can develop the efficiency of electrodeposition process of

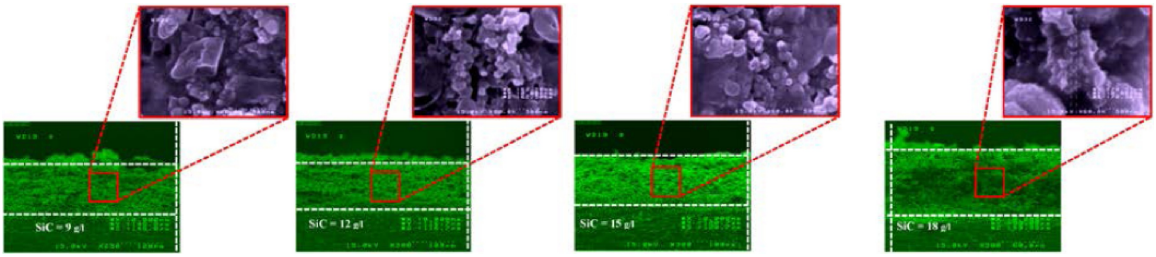

Figure 3 : Cross-sectional view and coating thicknesses of Ni–SiC–Gr nanocomposite coatings deposited at different SiC concentrations in electrolyte

nickel based nanocomposite coatings.

In order to understand the influence of reinforcement contents (SiC and Gr) on the microstructure and properties of composite coatings, several Ni–SiC–Gr nanocomposite coatings deposited at various electrolyte with different SiC concentrations (9, 12, 15, and 18 g/l) (Figure 5). This picture shows the variation of SiC and Gr contents in the nickel composite coatings as a function of SiC nanoparticles concentrations in the electrolytic bath (9, 12, 15, and 18 g/l). The weight percentage (wt.%) of SiC and Gr in the composite coatings (co-deposited using similar electrodeposition parameters) significantly increases with increasing SiC contents in the electroplating bath. It seems that the wt.% Gr particles in the coatings were decreased by increasing extra SiC contents in the electrolyte. It is clear that attendance of greater SiC contents in bath solution leads to absorbing higher reinforcement's particles (SiC) in coatings.

Microhardness analysis

The microhardness of coatings as a function of varied bath concentrations is presented in Figure 6. This figure shows the microhardness of Ni–SiC–Gr

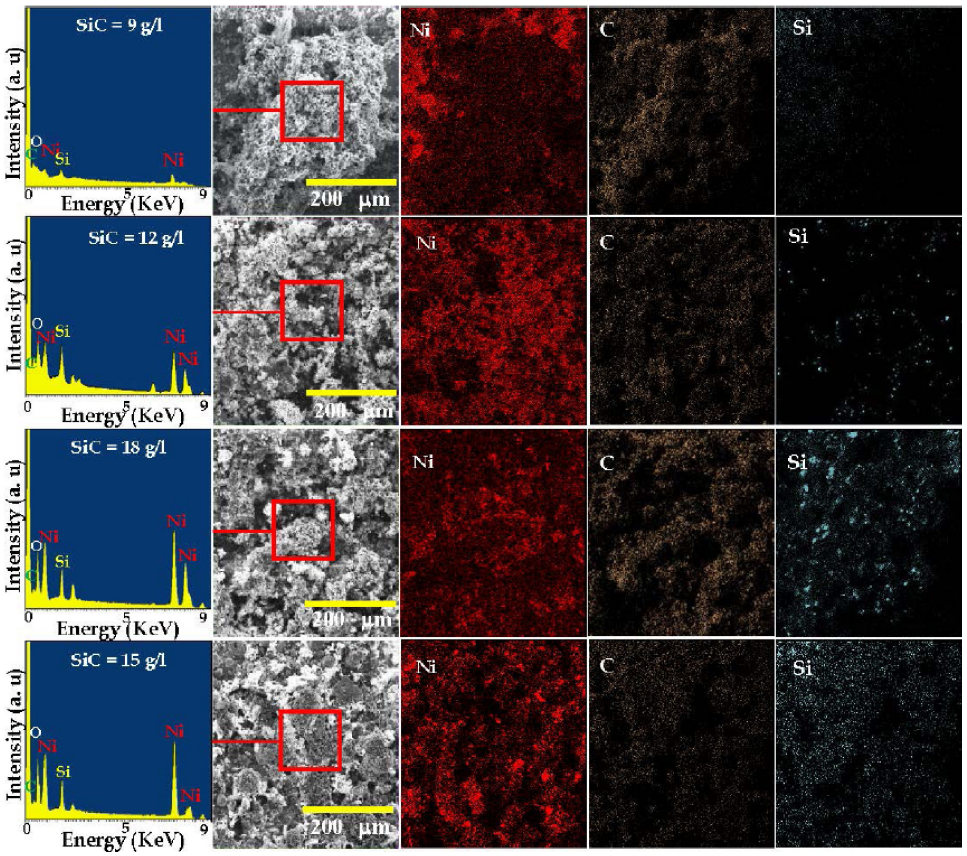

Figure 4 : EDS and elemental mapping spectra of Ni–SiC–Gr nanocomposite coatings deposited at diverse SiC concentrations in electrolyte

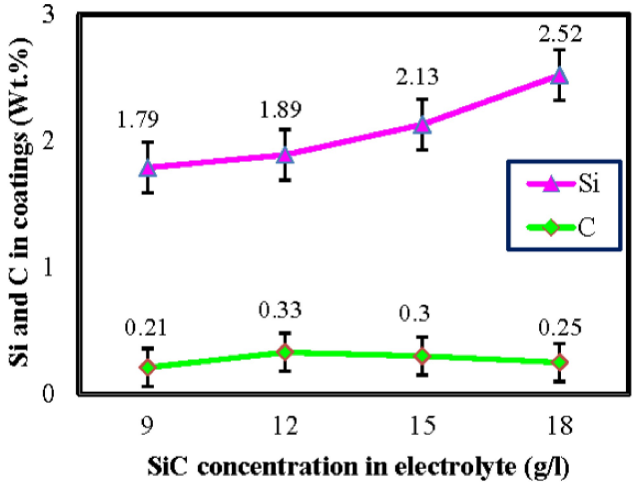

Figure 5 : Reinforcement content in the Ni–SiC–Gr nanocomposite coatings as a function of different SiC concentrations in electrolyte

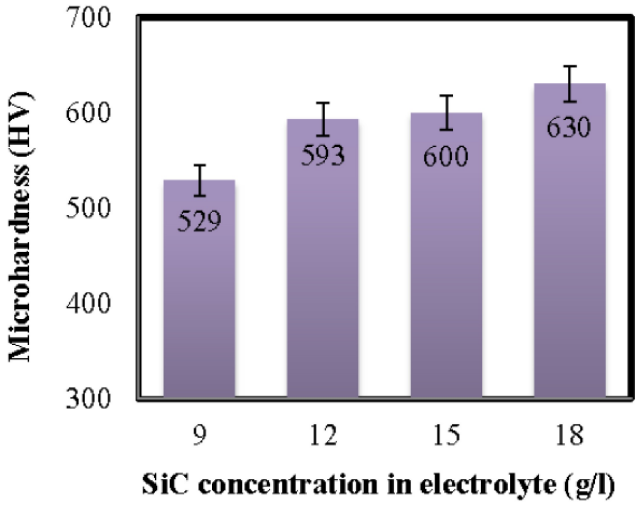

Figure 6 : Variation of microhardness of Ni–SiC–Gr nanocomposite coatings deposited at diverse SiC concentrations in electrolyte

nanocomposite coatings deposited at diverse SiC concentrations in the electrolyte (9, 12, 15, and 18 g/l). As might be expected, increasing the particle concentrations in electrolyte results in an increase in the number of nanoparticles in the deposited layer which should led to higher microhardness (630 Hv). It should be mentioned that the SiC particles deposited in nickel-based thin films are as obstacles versus the growth of the Ni grains and the plastic deformation of the matrix. The results are in good agreement with the microscopic observation and EDS analysis.

CONCLUSION

The influence of different bath concentrations on the morphological and microhardness features of Ni–SiC–Gr nanocomposite coatings on St–37 substrate was investigated. The effects varied SiC values in electrolyte were evaluated to optimize high quality coatings with suitable microhardness and morphological features. According to the XRD results, the significant peaks in the specimens were nickel and SiC phases which were almost similar in all the coatings deposited at different bath circumstances. Based on SEM and FE-SEM observations, a cluster like structure with an average particle size of about 62 nm was observed. The results, moreover, revealed that the optimum bath solution to deposit nickel-based nanocomposite coatings with harder surface was the electrolyte of 18 (g/l) SiC. Also, the depositions were controlled to obtain a specific thickness between 40 and 200 μm; thus, the thickness of coating at optimum bath plating conditions was acquired 99 μm. Eventually, the coating prepared at optimum bath conditions illustrated maximum microhardness about 630 HV which was in accordance with the SEM and EDS results.

ACKNOWLEDGMENT

The authors are grateful to research affairs of Islamic Azad University, Najafabad Branch for supporting this research.

REFERENCES

[1] D.Chaliampalias, G.Vourlias, E.Pavlidou, S.Skolianos, K.Chrissafis, G.Stergioudis; Appl.Surf.Sci., **255**, 3605 **(2009)**.
[2] V.Vitry, A.F.Kanta, F.Delaunois; Mater.Des., **39**, 269 **(2012)**.
[3] V.Vitrya, A.F.Kanta, F.Delaunois; Mater.Sci.Eng.B., **175**, 266 **(2010)**.
[4] B.Ramezanzadeh, M.M.Attar; Mater.Chem.Phys., **130**, 1208 **(2011)**.
[5] J.X.Kang, W.Z.Zhao, G.F.Zhang; Surf.Coat. Technol., **203**, 1815 **(2009)**.
[6] P.Sahoo, S.K.Das; Mater.Des., **32**, 1760 **(2011)**.
[7] S.C.Tjong, H.Chen; Mater.Sci.Eng.R., **45**, 1 **(2004)**.
[8] C.Suryanarayana, C.C.Koch; Hyperfine.Interact., **130**, 5 **(2000)**.
[9] P.Gyftou, M.Stroumbouli, E.A.Pavlatou, P.Asimidis, N.Spyrellis; Electrochim.Acta., **50**, 4544 **(2005)**.
[10] C.Zanella, M.P.Lekka, L.Bonora; J.Appl. Electrochem., **39**, 31 **(2009)**.
[11] E.Broszeit; Thin.Solid.Films., **95**, 133 **(1982)**.
[12] I.Garcia, J.Fransaer, J.P.Celis; Surf.Coat.Technol., **148**, 171 **(2001)**.
[13] M.Surender, B.Basu, R.Balasubramaniam; Tribol. Int., **37**, 743 **(2004)**.
[14] V.V.N.Reddy, B.Ramamoorthy, N.P.Kesava; Wear., **239**, 111 **(2000)**.
[15] F.B.Bahaaideen, M.R.Zaidi, A.A.Zainal; J.Sci.Ind. Res., **69**, 830 **(2010)**.
[16] Y.Wu, B.Shen, L.Liu, W.Hu; Wear., **261**, 201 **(2006)**.
[17] S.K.Kim, H.J.Yoo; Surf.Coat.Technol., **108**, 564 **(1998)**.
[18] Z.X.Niu, F.H.Cao, W.Wang, Z.Zhang, J.Q.Zhang, C.N.Cao; Met.Soc.China., **17**, 9 **(2007)**.
[19] M.D.Ger; Mater.Chem.Phys., **87**, 67 **(2004)**.
[20] M.C.Choua, M.D.Ger, S.T.Ke, Y.R.Huangc, S.T.Wu; Mater.Chem.Phys., **92**, 146 **(2005)**.
[21] A.Hovestad, L.J.J.Janssen; J.Appl.Electro., **25**, 519 **(1995)**.
[22] S.C.Wang, W.C.J.Wei; Mater.Chem.Phys., **78**, 574 **(2003)**.
[23] F.Hu, K.C.Chan; Appl.Surf.Sci., **233**, 163 **(2004)**.
[24] R.Elansezhian, B.Ramamoorthy, P.Kesavan Nair, Surf.Coat.Tech., **203**, 709 **(2008)**.
[25] L.Burzynska, E.Rudnik, J.Koza, L.C.Blaz, W.Szymanski; Surf.Coat.Tech., **202**, 2545 **(2008)**.
[26] M.R.Vaezi, S.K.Sadrnezhaad, L.Nikzad; Colloids. Surf.A., **315**, 176 **(2008)**.
[27] T.Borkar, S.P.Harimkar; Surf.Coat.Tech., **205**, 4124 **(2011)**.
[28] Z.Liao, Z.Huang, H.Hua, Y.Zhang, Y.Tan; Bioresource.Technol., **102**, 7953 **(2011)**.
[29] M.A.Siddig, S.Radiman, S.V.Muniandy, L.S.Jan; Colloids.Surf.A., **236**, 57 **(2004)**.
[30] A.M.Rashidi, A.Amadeh, J.Mater.Sci.Technol., **26**, 82 **(2010)**.
[31] P.Wang, Y.L.Cheng, Z.J.Zhang; Coat.Technol.Res., **8**, 409 **(2011)**.
[32] H.Gül, F.Kilic¸, S.Aslan, A.Alp, H.Akbulut; Wear., **267**, 976 **(2009)**.
[33] Y.N.Gou, W.J.Huang, R.C.Zeng, Y.Zhu; Trans. Nonferrous.Met.Soc.China., **20**, 674 **(2010)**.